

The Performance of Disc Cutters in Simulated Jointed Rock

D. F. HOWARTH

Research Associate, School of Mining Engineering, The University of New South Wales

SUMMARY A series of controlled laboratory experiments has been undertaken to assess the performance of disc cutters in simulated jointed rock. The disc cutters used (similar to those found on full face tunnelling machines) were mounted on a linear rock cutting rig capable of cutting at speeds up to 300 mm/s and sustaining thrust forces of up to 100 kN. The simulated jointed rock test samples consisted of rectangular blocks of sandstone clamped together. The parameters measured to assess disc performance were thrust, rolling and lateral forces on the cutting tool together with a quantitative assessment of the size and mass of debris produced. Several types of experiment were undertaken in order to ascertain both fundamental and practical aspects of cutting in jointed rock. These experiments involved varying joint width, joint spacing, overburden pressure, tool spacing and the angle of attack of the cutting tool relative to the joint planes. The results show the effects of jointed rock masses on cutting tool forces, energy involved in cutting and the size of debris produced. In addition a mechanism is proposed to explain the low strength characteristics of jointed rock.

NOTATION

D	disc diameter	mm
C	confining load	t
C.I.	coarseness index	-
F_L	mean lateral force	kN
F_R	mean rolling force	kN
F_T	mean thrust force	kN
P	penetration	mm
Q	yield	m^3/km
S.E.	specific energy	MJ/m^3
T	joint width/thickness	mm
V	velocity	mm/s
X	block width or spacing between joints	mm
σ_c	uniaxial compressive strength	MPa
θ_c	breakout angle	degrees
ϕ	disc edge angle	degrees
ψ	angle of attack (angle of joint plane relative to line of action of disc cutter)	degrees

1 INTRODUCTION

The performance of disc cutters of varying geometries in continuous rock has been well established (Roxborough and Phillips, 1975a) and (Ozdemir, Miller and Wang, 1977). However, little or no work has been undertaken to assess the performance of disc cutters in jointed rock. (It should be stated here that for the purposes of this paper jointed rock is defined as a series of regular blocks of rock, artificially separated to give open joints or fissures of known regular dimensions.)

It is generally accepted that under most circumstances jointed rock is weaker than a comparable block of solid rock. However, no quantitative assessment of the forces and energy required to excavate jointed rock has been made. This information may have a practical application when designing disc arrays for a tunnelling machine head when cutting in areas with preferred joint directions.

Mathematical models that have been proposed to predict the disc forces required to penetrate continuous rock are not applicable for a comparable

situation in jointed rock. The mechanism of failure of jointed rock under the action of a disc cutter is complex and difficult to quantify.

2 ROCK CUTTING RIG AND INSTRUMENTATION

2.1 Cutting Rig

The cutting rig used in these experiments was an extensively modified planing machine shown in Figure 1. This machine is capable of accepting large blocks of rock, has variable cutting speed and is robust enough to sustain static and dynamic thrust forces (vertical) up to 100 kN.

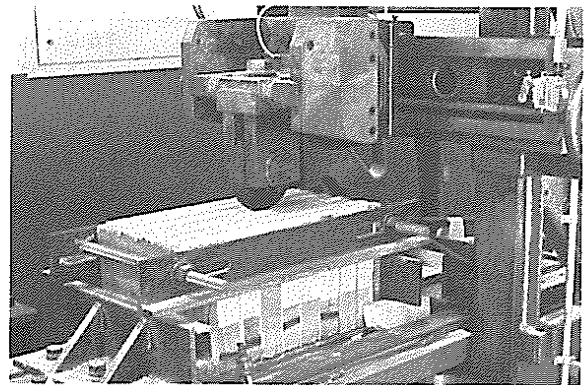


Figure 1 Rock cutting rig

In this system the cutting tool remains stationary while the rock sample is passed beneath it. The table is driven by a 7.5 kW induction motor which in turn is controlled by an AC variable frequency inverter which allows the speed of the table to be continuously varied from 50-300 $\text{mm}\cdot\text{s}^{-1}$. Rock samples of approximately 450mm x 450mm x 350mm are mounted on the table and clamped firmly prior to cutting. The individual blocks of rock comprising the jointed rock mass were cut from large samples using a diamond saw, blocks were separated using a low strength material such as paper, care being taken when assembling the units to ensure that the media used for separating the blocks was below the

penetration level of the cutting tool. This ensured that the disc cut through open joints. A confining load was provided in a line parallel to the direction of motion of the table by a hydraulic power pack capable of providing loads up to 10t. A tensioned framework, also shown in Figure 1, was provided to give a degree of lateral constraint. The rig also has the facility to dress rock samples prior to cutting.

2.2 Mode of Operation and Instrumentation

The experimental procedure involved setting the experimental variables such as confining load and penetration then passing the block beneath the cutting tool. Thrust, rolling and lateral forces were continually monitored during the experiment. At the end of each cut, the length of cut was recorded, debris collected and a screen analysis undertaken.

Instrumentation included a triaxial dynamometer, shown in Figure 1, (O'Dogherty and Whittaker, 1965) capable of resolving the force acting on the disc into three orthogonal components. Signals are sent from the dynamometer via dynamic strain amplifiers to a microprocessor based data acquisition and mini computer facility described in detail by Howarth (1978). Data is stored in digital form on flexible magnetic discs for future analysis.

3 TEST MATERIAL

The experimental programme was conducted in Gosford Summersby Sandstone and has the measured properties detailed in Table 1.

TABLE 1

PROPERTIES OF GOSFORD SUMMERSBY SANDSTONE

Grain size mm	0.7
Quartz content %	34
Unconfined compressive strength MPa	42.3±2.56(A)*
Unconfined tensile strength MPa	2.84±0.36(B)*
Unconfined shear strength MPa	14.5±1.62(C)*
Static Young's Modulus GPa	9.62±2.47(D)*
Schmidt rebound number	47.4±6.43(E)*
Dry mass density kg/m ³	2200±61

*Mean value of property in two directions, one at right angles to the other

- A. 20 samples, cylinders 54.2mm dia.x 108.3mm long
- B. 10 samples, discs 40.6mm dia.x 19.8mm long
- C. 10 samples, cylinders 40.7mm dia.x 78.5mm long
- D. Tangent modulus, 10 samples dimensions as A.
- E. 125 values

4 EXPERIMENTAL PROGRAMME & DESIGN OF EXPERIMENTS

4.1 Experimental Programme

Six major experiments were undertaken to establish the effect of jointed rock masses on the performance of disc cutters, each variable having five levels in arithmetic progression and each individual test within an experiment repeated four times to obtain mean values (Roxborough and Phillips, 1975b). A series of preliminary experiments was undertaken to assess the levels of variables to be used in the main experimental programme. It was found that as disc diameter increased the damage to the jointed blocks also increased. Therefore in an effort to minimise damage and preserve the integrity of the jointed blocks the smallest diameter disc, namely 100mm, was chosen for the entire series of experiments. The experiments are detailed in Table II.

TABLE II
EXPERIMENTAL PROGRAMME

Exp* No.	Parameters under Investigation	Constants	Variables	Level of Variables	Type of Exp.
1	F _T , F _R , Q, SE (1. For validation of rock cutting system 2. For comparison with jointed rock experiments.)	D = 100mm V = 50mm/s	P φ	2, 4, 6, 8, 10mm 30, 45, 60, 75, 90°	a
2	F _T , F _R , Q, SE	D = 100mm X = 60mm V = 50mm/s ψ = 90°	P φ C T	2, 4, 6, 8, 10mm 30, 45, 60, 75, 90° 2, 4, 6, 8, 10 t 0, 0.75, 1.5, 2.25, 3.0mm	b
3	F _T , F _R , Q, SE	D = 100mm C = 6 t V = 50mm/s ψ = 90° P = 6mm φ = 60°	X T	20, 40, 60, 80, 100mm 0, 0.75, 1.5, 2.25, 3.0mm	a
4	F _T , F _R , Q, SE	D = 100mm C = 6 t V = 50mm/s X = 60mm P = 6mm	ψ φ	30, 45, 60, 75, 90° 30, 45, 60, 75, 90°	a
5	Q, SE, CI	X = 60mm C = 6 t V = 50mm/s ψ = 90° T = 1.50mm P = 6mm D = 100mm φ = 60°	S/P	2, 4, 6, 8, 10, 15, 20	c
6	Q, SE, CI (For comparison with Exp. 5)	φ = 60° P = 6mm D = 100 mm V = 50mm/s	S/P	2, 4, 6, 8, 10, 15, 20	c

* Experiment 1 and 6 in solid rock
Experiments 2 to 5 in jointed rock

a - two variable, full factorial
b - partial factorial
c - one variable, full factorial

4.2 Design of Experiments

Experiment 2 was a partial factorial experiment based on a method proposed by Protodykanov and Teder (1970) whereby experiments are chosen systematically from an experimental matrix based on orthogonal Latin squares. Essentially the method allows a comparison of a parameter with a variable at mean values of the other variables in the experiment. The remaining experiments are either single or two variable experiments as indicated in Table II.

4.3 Disc Cutting Parameters

The parameters of disc performance are defined as follows :-

- 1) Thrust force F_T - the average force required to be applied vertically to effect a prescribed penetration.
- 2) Rolling force F_R - the average force required to be applied in the direction of motion of the cutting tool to effect a prescribed penetration.
- 3) Yield Q - the volume of rock excavated per unit distance cut.
- 4) Specific energy SE - the work done per unit volume of rock excavated.
- 5) Coarseness index CI - a measure of the debris size from an excavated cut. This is a dimensionless number, being the sum of the cumulative mass percentages recorded in the screen analyses (Barker, 1964).

The mean lateral force F_L was monitored for all experiments and was found to be sensibly zero, and hence no further reference is made to this parameter.

5 VALIDITY OF ROCK CUTTING SYSTEM

5.1 Experimental Results

It was deemed necessary to carry out rock cutting experiments similar to those undertaken elsewhere (Roxborough and Phillips, 1975a) in order to establish the validity of the rock cutting system. The results of this experiment (Experiment 1, Table II) are shown in Figure 2.

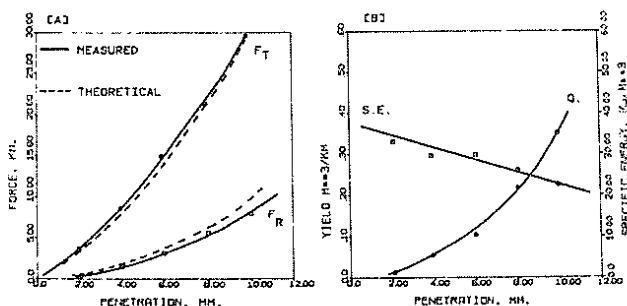


Figure 2 Comparison of measured and theoretical values in unjointed rock (Exp. 1)

$$\phi = 60^\circ$$

The results show the same trends as reported elsewhere. Furthermore, Figure 2A shows that the measured and theoretical values of F_T and F_R are in close agreement. The theoretical values are calculated from the equations proposed by Roxborough and Phillips (1975a).

$$F_T = 4 \sigma_c \tan \frac{\phi}{2} \sqrt{DP^3 - P^4} \quad (1)$$

$$F_R = 4 \sigma_c P^2 \tan \frac{\phi}{2} \quad (2)$$

Figure 2B shows the yield to increase as the square of the penetration and is described by the equation

$$Q = P^2 \tan \theta \text{ (per unit distance cut)} \quad (3)$$

where θ is the breakout angle of the rock and is equal to 72° . Again this is in accordance with work undertaken elsewhere.

6 EXPERIMENTAL RESULTS IN JOINTED ROCK

6.1 Effect of Penetration

The effect of penetration on F_T and F_R is shown in Figure 3A.

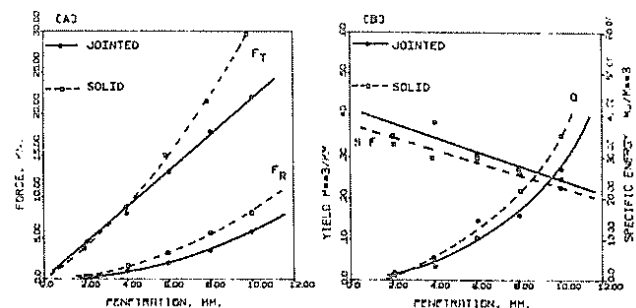


Figure 3 Effect of penetration (Exp. 2)
 $\phi = 60^\circ$, $T = 1.5\text{mm}$, $C = 6\text{t}$

Both F_T and F_R increase with increasing penetration and follow similar trends as shown by an identical disc in solid rock. There is close agreement in solid and jointed rock forces at low penetration however, as penetration increases so does the discrepancy between the forces. At a penetration of 10mm the difference between F_T (solid) and F_T (jointed) is approximately 25 percent.

Figure 3B, shows the curves for solid and jointed rock for both yield and specific energy to be in close agreement in both trend and magnitude. These results appear to be anomalous; it was reasonable to expect that the yield would be higher in the case of jointed rock as a result of end chips being formed at the air/rock interfaces. The specific energy appears to be anomalously high, this is a direct consequence of the lower yield. These apparently anomalous results are being investigated further.

6.2 Effect of Edge Angle

Thrust and rolling forces increase with increasing edge angle as shown in Figure 4A.

The trends for jointed and solid rock are similar. At small edge angles the discrepancy between jointed and solid rock forces is negligible, however, as edge angle increases the discrepancy increases and in the case of F_T , at $\phi = 90^\circ$, this discrepancy is approximately 36%. These results together with the similar result reported in 6.1 suggests that jointed rocks should be excavated with high edge angle discs at high penetrations to obtain maximum cutting efficiency.

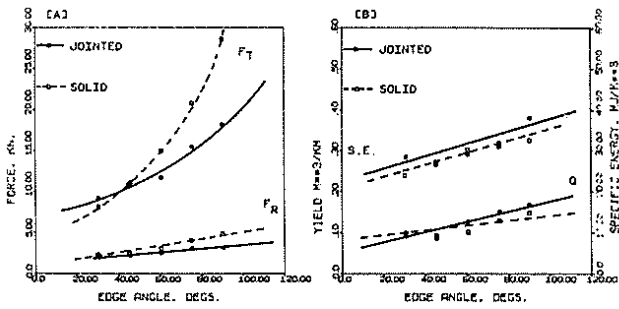


Figure 4 Effect of edge angle (Exp. 2)
 $P = 6\text{mm}$, $T = 1.50\text{mm}$, $C = 6t$

Figure 4B, shows both yield and specific energy increasing with increasing edge angle. The results do not indicate any significant difference between the magnitudes of yield and specific energy when compared to an identical situation in solid rock.

6.3 Effect of Confining Load

The confining load was applied in a direction normal to that of the joint planes. The effect of confining load on F_T and F_R is shown in Figure 5A.

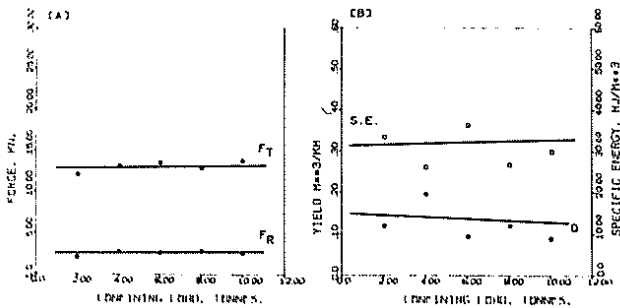


Figure 5 Effect of confining load (Exp. 2)
 $P = 6\text{mm}$, $T = 1.50\text{mm}$, $\phi = 60^\circ$

Thrust and rolling force are marginally affected by confining load.

Figure 5B, shows a reduction in yield and corresponding increase in specific energy with increasing confining load. However, as the data is scattered it is suggested that in actual fact yield and specific energy are only marginally affected by confining load. The maximum load (10 tonnes) that could be applied to the jointed mass represents a confining stress of less than 5% of the ultimate compressive strength, however it was not technically possible to increase the load further. It is possible that loads in excess of 10 tonnes may have an effect on the parameters shown in 5A and 5B.

6.4 Effect of Joint Width

Joint width is the distance between two adjacent blocks of rock and was created by inserting low strength media between the blocks. The effect of joint width on F_T and F_R is shown in Figure 6A. Rolling force is unaffected by joint width however, thrust force decreases with increasing joint width. This is partially due to the increasing reduction in disc area in contact with the rock as joint width increases. A further mechanism to explain this reduction in force is discussed in detail in section 7.

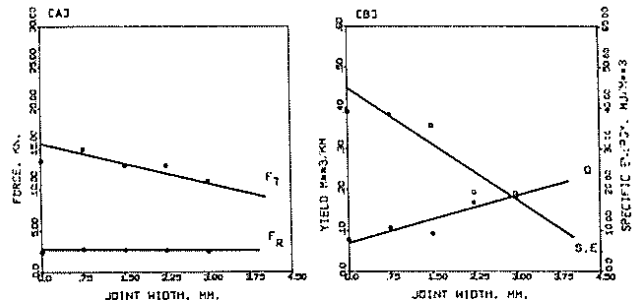


Figure 6 Effect of joint width (Exp. 2)
 $P = 6\text{mm}$, $\phi = 60^\circ$, $c = 6t$

Figure 6B, shows the yield increasing the increasing joint width. This is a result of larger end chips being formed as the joint width increases. The specific energy shows a significant decrease with increasing joint width. Thus cutting efficiency increases with increasing joint width.

6.5 Effect of Block Width

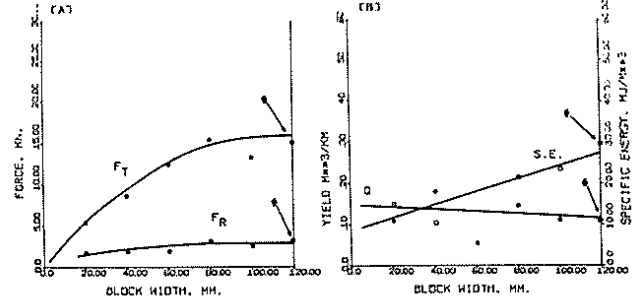


Figure 7 Effect of block width (Exp. 3)
 $T = 1.50\text{mm}$ # These points extracted from Exp. 1, i.e. Block width $\rightarrow \infty$ (solid rock)

Figure 7A, shows F_T and F_R increasing with increasing block width to a point where both force curves become parallel with the X axis. This occurs at a block width of 100-120mm, at which point the jointed rock can be regarded as a continuous mass. Furthermore, the values of F_T and F_R at this point are in close agreement with those obtained in solid rock.

Yield decreases with increasing block width as shown in Figure 7B. This is due to the smaller weaker blocks producing larger end chips. Specific energy increases with increasing block width, implying that excavation is more efficient in ground comprising of small blocks. Both curves tend towards values obtained in solid rock, however, due to the scatter of the data, the point at which the jointed rock approximates the behaviour of a solid rock cannot be defined.

6.6 Effect of Block to Joint Width Ratio

Further analysis of the data obtained in Experiment 3 yields the graphs shown in Figure 8. The points on the graph represent the ratio, block width divided by joint width plotted against the relevant parameter for all tests conducted.

These results confirm those reported in Section 6.5. The limiting value of X/T (where the parameter becomes parallel with the X axis) is approximately 80. At this point the value of the parameter approximates the value obtained in solid rock.

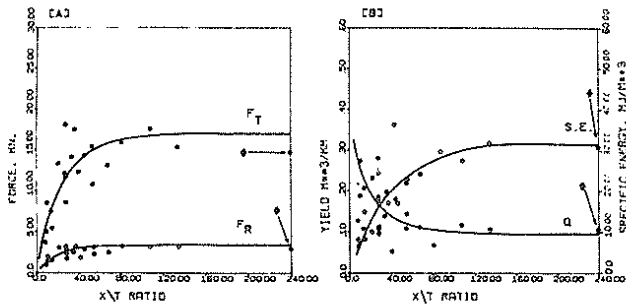


Figure 8 Effect of block width to joint width ratio (Exp. 3)

These points extracted from Exp. 1, i.e. Block width $\rightarrow \infty$ (solid rock)

6.7 Effect of Angle of Attack

Angle of attack is defined as the angle of the joint plane relative to the line of action of the disc cutter. An angle of attack of 90° is defined as the disc is cutting normal to the direction of the joint planes. The effect of angle of attack is shown in Figure 9.

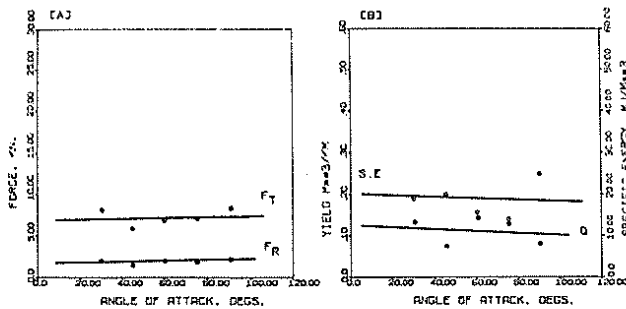


Figure 9 Effect of angle of attack (Exp. 4)

$\phi = 45^\circ$

The effect of angle of attack on thrust and rolling force, yield and specific energy is negligible. For practical purposes it may be stated that the parameters are only marginally affected by angle of attack.

6.8 Effect of Tool Spacing

Disc cutters do not generally operate in isolation, normally they are disposed in an array on the cutting head of the tunnelling machine. It is, therefore, useful to know at what distance to space cutting tools in the array. In this experiment discs were spaced at set distances from previously excavated grooves.

The most useful parameters available when assessing the effect of spacing, are those which involve the mass of rock created by cutting. These are namely yield, specific energy and coarseness index. The effect of spacing on these parameters for both solid and jointed rock are shown in Figure 10. The trends of these curves are in close agreement with other published experimental data (Roxborough and Phillips, 1975a).

Figure 10A, shows jointed rock yield to rise rapidly as tool spacing increases. The yield reaches a maximum at a spacing of approximately 40mm, this corresponds to a S/P (spacing to penetration) ratio of 6.6, a sharp decrease follows

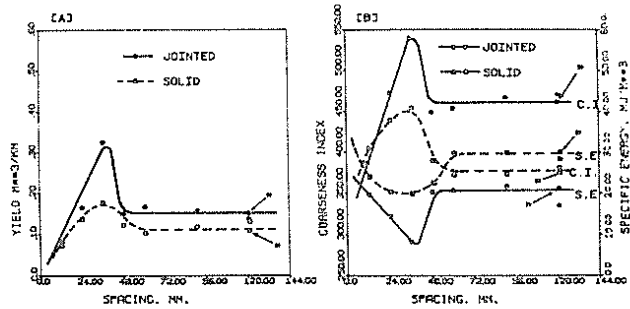


Figure 10 Effect of tool spacing (Exp. 5 and 6)

$P = 6 \text{ mm}, \phi = 60^\circ$

* data points taken from unrelieved cutting experiments 1 and 2

and the curve levels off at a S/P ratio of approximately 9.0. At this point the cutter is operating in isolation, or in the unrelieved situation.

Figure 10B, shows coarseness index to have a maximum value (coarse debris-large chips) at a S/P ratio of 6.4 and levelling out at a S/P ratio of 9.0. The specific energy curve indicates that the cutter reaches peak efficiency at an S/P ratio of 6.4 and levels out at an S/P ratio of 9.0.

Maximum disc interaction is indicated at a S/P ratio of approximately 6.5. This was observed during the experimental work, when the disc spacing was set close to a value corresponding to an S/P ratio of 6.5 relatively large slabs of rock were observed to break out between adjacent disc grooves. Interaction between discs was observed to stop at a S/P ratio of 9-10, at this ratio and higher ratios the cutters operate in isolation.

The differences between the optimum and 'cut-off' S/P ratios for solid and jointed rock are marginal as shown in Table III.

TABLE III
OPTIMUM AND 'CUT-OFF' S/P RATIOS
IN SOLID AND JOINTED ROCK

Rock Type	S/P Ratio	
	Optimum	'Cut-off'
Jointed Rock (Exp. 5)	6.5	9.0
Solid Rock (Exp. 6)	5.9	11.0

$P = 6 \text{ mm}, \phi = 60^\circ$

It is apparent that in relieved cutting in jointed rock shear failure between adjacent grooves is the predominant mechanism of failure and the formation of end chips has very little effect.

7 A POSSIBLE MECHANISM TO EXPLAIN THE LOW STRENGTH CHARACTERISTICS OF JOINTED ROCK

Figure 3A shows that at a penetration of 10mm the difference in F_T (solid) and F_T (jointed) is approximately 25%. Equation (1) can be used to calculate the thrust force required to penetrate solid rock, the reduction in thrust force due to the decrease in projected disc surface area contact can be found by using the equation

$$F_T = \sigma_c \left(\left[4 \tan \frac{\phi}{2} \sqrt{DP^3 - P^4} \right] - \left[2PT \tan \frac{\phi}{2} \right] \right) \quad (4)$$

The function $2PT \tan \frac{\phi}{2}$ is the projected area of disc contact over one open joint. For the purposes of the following calculation the disc is assumed to cut one open joint and to have its centre lie over the centre of the joint.

If values of ϕ , D and T are extracted the experimental conditions ($P = 10\text{mm}$) shown in Figure 3A and substituted in equation (4) the reduction in thrust force as a result of the reduction in projected disc surface area in contact with the rock can be shown to be 2.5%.

It is evident that the reduction in thrust force required to excavate the rock is not wholly attributable to the reduction in projected area of disc contact area with the rock. Equations (1) and (4) assume that the rock is broken under the action of compressive forces, it is suggested that some other mode or modes of failure operate when discs cut jointed rock. Furthermore, it is suggested that when a disc penetrates a jointed block the block expands or dilates at right angles to the direction of application of the applied stress (the Poisson effect). Consequently inter-particle tensile stresses are set up and therefore the rock under the disc may fail partly in tension. Taking this concept one step further it is possible to explain the decreasing strength of rock with decreasing block width as shown in Figure 7A. When a disc penetrates a block the block is deformed and strained. It is suggested that if the deformation remains constant, as block width increases the degree of strain decreases, therefore decreasing the tendency of the rock to fail in tension and hence increasing the force required to excavate the rock. Investigations are presently being undertaken to investigate this mechanism further.

8 CONCLUSIONS

The following conclusions relate to the experimental conditions discussed in this paper.

1. The rock cutting system described produces data from cutting continuous rock that is in close agreement with other published experimental data.
2. To achieve maximum effectiveness when cutting in jointed rock disc cutters should have large edge angles and cut at high penetrations.
3. Cutting efficiency increases with increasing joint width.

4. Cutting efficiency decreases with increasing block width.
5. When the block width to joint width ratio exceeds 80 the jointed rock behaves as a continuous mass.
6. Angle of attack and confining load have little or no measurable effect on the performance of disc cutters in jointed rock.
7. The optimum and 'cut-off' S/P ratios are in close agreement to those of solid rock.

9 ACKNOWLEDGEMENTS

The equipment used in this work was provided by a grant from the Australian Research Grants Committee.

The author wishes to thank Dr. H.R. Phillips, Lecturer in the School of Mining Engineering, The University of New South Wales, for his assistance in the preparation of this paper.

10 REFERENCES

- BARKER, J.S. (1964). A laboratory investigation of rock cutting using large picks. Int. J. Rock Mech. Mining Sci. Vol. 1, pp519-534.
- HOWARTH, D.F. (1978). Tunnelling machine research at The University of New South Wales. Symp. Rock Breaking Equipment and Techniques, Melbourne, pp43-49.
- O'DOHERTY, M.J. and WHITTAKER, D. (1965). An examination of the characteristics of a solid plate dynamometer designed for triaxial force measurements. N.C.B./M.R.E. Technical Memorandum, U.K., No. 197.
- OZDEMIR, L., MILLER, R. and WANG, F.D. (1977). Mechanical tunnel boring, prediction and machine design. Annual Report, Colorado School of Mines.
- PROTODYAKANOV, M.M. and TEDER, R.I. (1970). Rational methods of planning experiments. Dynamic Rock Mechanics (Ed. G.B. Clark) Twelfth Symp. on Rock Mech.: Univ. Missouri, Rolla, pp129-149.
- ROXBOROUGH, F.F. and PHILLIPS, H.R. (1975a). Rock excavation by disc cutter. Int. J. Rock Mech. Min. Sci. and Geomech. Abstr. Vol. 12, pp361-366.
- ROXBOROUGH, F.F. and PHILLIPS, H.R. (1975b). The mechanical properties and cutting characteristics of the Bunter Sandstone. Report to T.R.R.L., Univ. of Newcastle upon Tyne, U.K., 292 pp.